Supporting Information

Pfleger *et al.* 10.1073/pnas.0808118105

SI Methods: Cloning, Mutagenesis, and Protein Purification

Preparation of AsbF for Enzymatic Assays. The *asbF* gene of *B. anthracis* Sterne strain was cloned into the expression vector pMCSG7 (Midwest Center for Structural Genomics) by using ligation-independent cloning (LIC) (1). The pMCSG7 vector, bearing a TEV protease cleavage site, creates a construct with a cleavable His_6 tag fused into the N terminus of the target protein with three artificial residues (SerAsnAla). Site-directed mutagenesis was performed on this construct in modification of a Stratagene QuikChange protocol: Primers containing the desired mutation were kept at a constant concentration while varying amounts of template DNA were titrated. Ten units of Phusion DNA polymerase (Finnzymes) was used per 50-μL reaction. Reactions shown by gel electrophoresis to contain amplified vector were incubated with 10 units of DpnI (New England Biolabs) for 2 h to remove template and were used to transform chemically competent XL1-Blue cells for amplification. All DNA manipulation was confirmed by DNA sequencing.

All pMCSG7-*asbF* constructs were transformed into Z-competent (Zymo Research) BL21 expression cells (Novagen). An overnight LB starter culture was used to inoculate 1 L (or in the case of point mutants, 250 mL) of Terrific Broth (TB) medium and shaken at 190 rpm at 37 °C until an OD_{600} of ≈1 was reached. Cultures were cooled to 18 °C over the course of 1 h and induced with 250 μM IPTG for incubation overnight. Resulting cell pellets were resuspended in 5 mL of lysis buffer (20 mM Hepes, pH 8.0/300 mM NaCl/20 mM imidazole/1 mM DTT/10% glycerol) per gram of pellet and lysed by sonication. Soluble lysate was incubated with preequilibrated Ni-NTA resin (Qiagen) for 3 h at 4 °C, poured through a glass column, washed with 6× the lysate volume of lysis buffer, and eluted with an imidazole solution (20 mM Hepes, pH 8.0/300 mM NaCl/300 mM imidazole/1 mM DTT/10% glycerol) into 1-mL fractions. The expected mass of 35 kDa was observed for the isolated His-tagged fusion protein (Fig. S7). Eluted fractions shown to contain enzyme and a minimal amount of contaminants were pooled, concentrated, and buffer-exchanged in an Amicon Ultra 30-kDa MW cutoff filter (Millipore) with 20 mM Hepes (pH 8.0), 20 mM NaCl, 1 mM DTT, and 10% glycerol. Protein concentration was determined by using A_{280} and Bradford assay, and then preparations were flash-frozen in liquid nitrogen and stored at −80 °C.

Preparation of AsbF for Crystallization. After failing to obtain diffraction quality crystals with the initial pMCSG7-*asbF* construct, *asbF* was cloned in pMCSG26 vector with two variations, including an uncleavable C-terminal His_6 tag and a C-terminal His_6 tag with a TEV protease cleavage site. The *asbF* gene was overexpressed in *E. coli* BL21 (DE3)-Gold (Stratagene) harboring an extra plasmid encoding three rare tRNAs (AGG and AGA for Arg, ATA for Ile).

Cell cultures were grown at 37 °C to an OD_{600} of ≈0.95, cooled down before adding Se-Met and 0.5 mM IPTG to induce, and maintained at 18 °C overnight. The harvested cells were lysed by sonication in the presence of 1 mg/mL lysozyme and a protease inhibitor mixture tablet (Complete; Roche) in 35 mL of lysis buffer containing 50 mM Hepes (pH 8.0), 500 mM NaCl, 10 mM imidazole, 10 mM 2-mercaptoethanol, and 5% vol/vol glycerol. The lysate was clarified by centrifugation at 30,000 × *g* (RC5C-Plus centrifuge, Sorval) for 75 min, followed by filtration through a 0.45-μm filter (Gelman) before loading onto a 5-mL Ni-Histrap column (GE Healthcare) for purification.

Protein was purified by two-step Ni-affinity chromatography following the standard protocol described previously (2). Immobilized metal affinity chromatography (IMAC-I) was conducted by using a 5-mL HiTrap Chelating HP column charged with Ni^{2+} ions and buffer-exchange chromatography on a HiPrep 26/10 desalting column (GE Healthcare) on ÄKTAxpress (GE Healthcare). Both AsbF expressed from the pMCSG26 vector with a TEV cleavage site and the protein with an N-terminal His_6 tag that could not be cleaved were dialyzed in crystallization buffer (20 mM Hepes, pH 8.0/250 mM NaCl/2 mM DTT) and concentrated to 82 mg/ml by using an Amicon Ultra centrifugal filter device (Millipore). For AsbF expressed from pMCSG26 vector with a TEV cleavage site, the His_6 tag was removed using recombinant TEV protease (a gift from D. Waugh, National Cancer Institute) in a 1:30 ratio by incubating at 4 °C for 72 h. The TEV protease cleavage left six artificial residues (ENLYFQ) remaining at the C terminus. The AsbF protein was then further purified by a 5-mL manually packed Ni-superflow affinity column (GE Healthcare). The protein eluted as a flow-through from the column in lysis buffer with 20 mM imidazole, was dialyzed in crystallization buffer containing 20 mM Hepes (pH 8.0), 250 mM NaCl, and 2 mM DTT, and concentrated to 85 mg/mL by using an Amicon Ultra centrifugal filter device (Millipore).

1. Stols L, *et al.* (2002) A new vector for high-throughput, ligation-independent cloning encoding a tobacco etch virus protease cleavage site. *Protein Expression Purif* 25:8–15.

2. Kim Y, *et al.* (2004) Automation of protein purification for structural genomics. *J Struct Funct Genomics* 5:111–118.

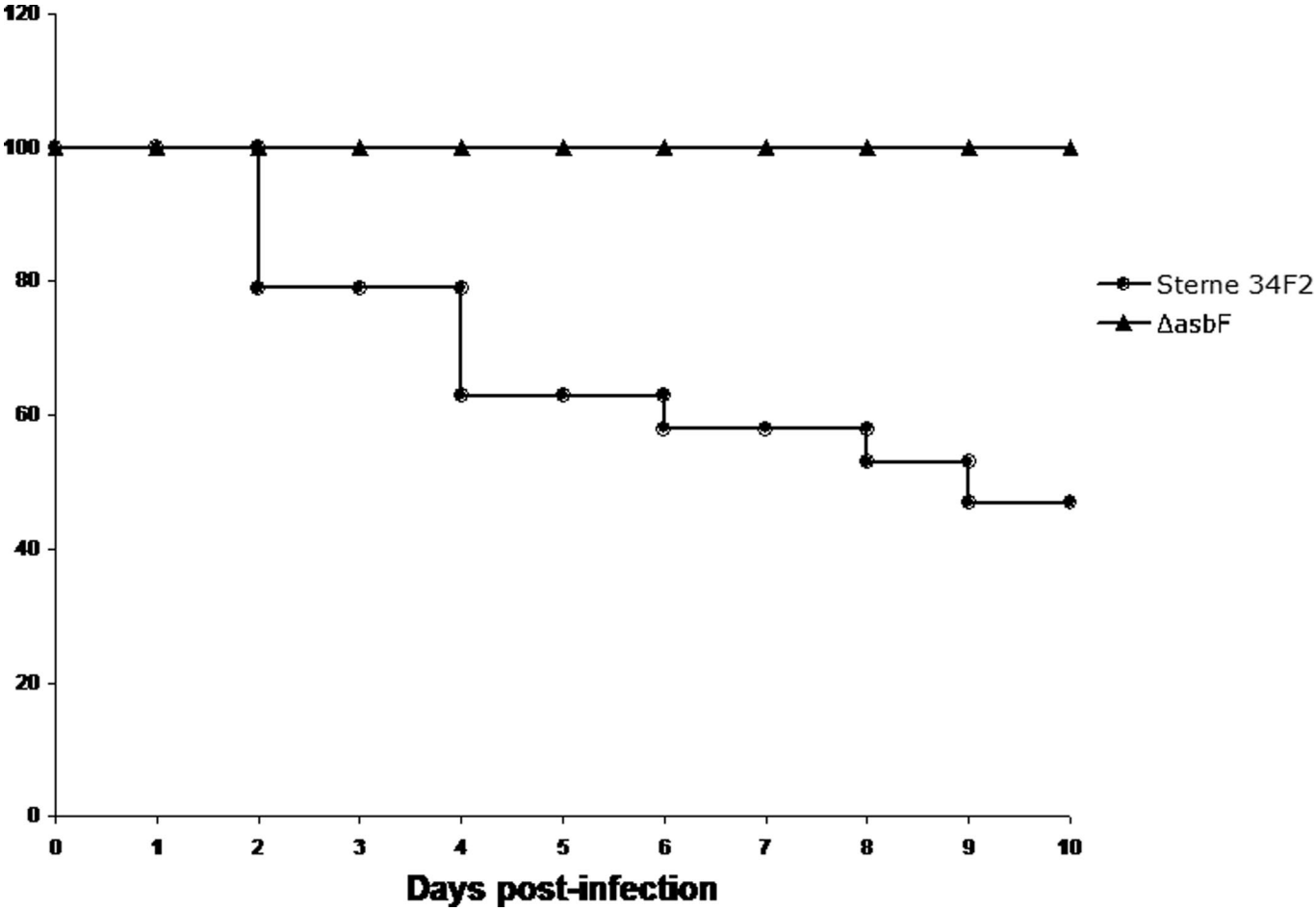

Fig. S1. Attenuation of virulence of the Δ*asbF* mutant of *B. anthracis* in mice. DBA/2 mice were inoculated with $\approx 1 \times 10^4$ spores of either the parental (Sterne 34F2) or mutant (Δ*asbF*) strain of *B. anthracis* via intratracheal injection. The group sizes were 19 mice (Sterne 34F2) and 20 mice (Δ*asbF*), respectively.

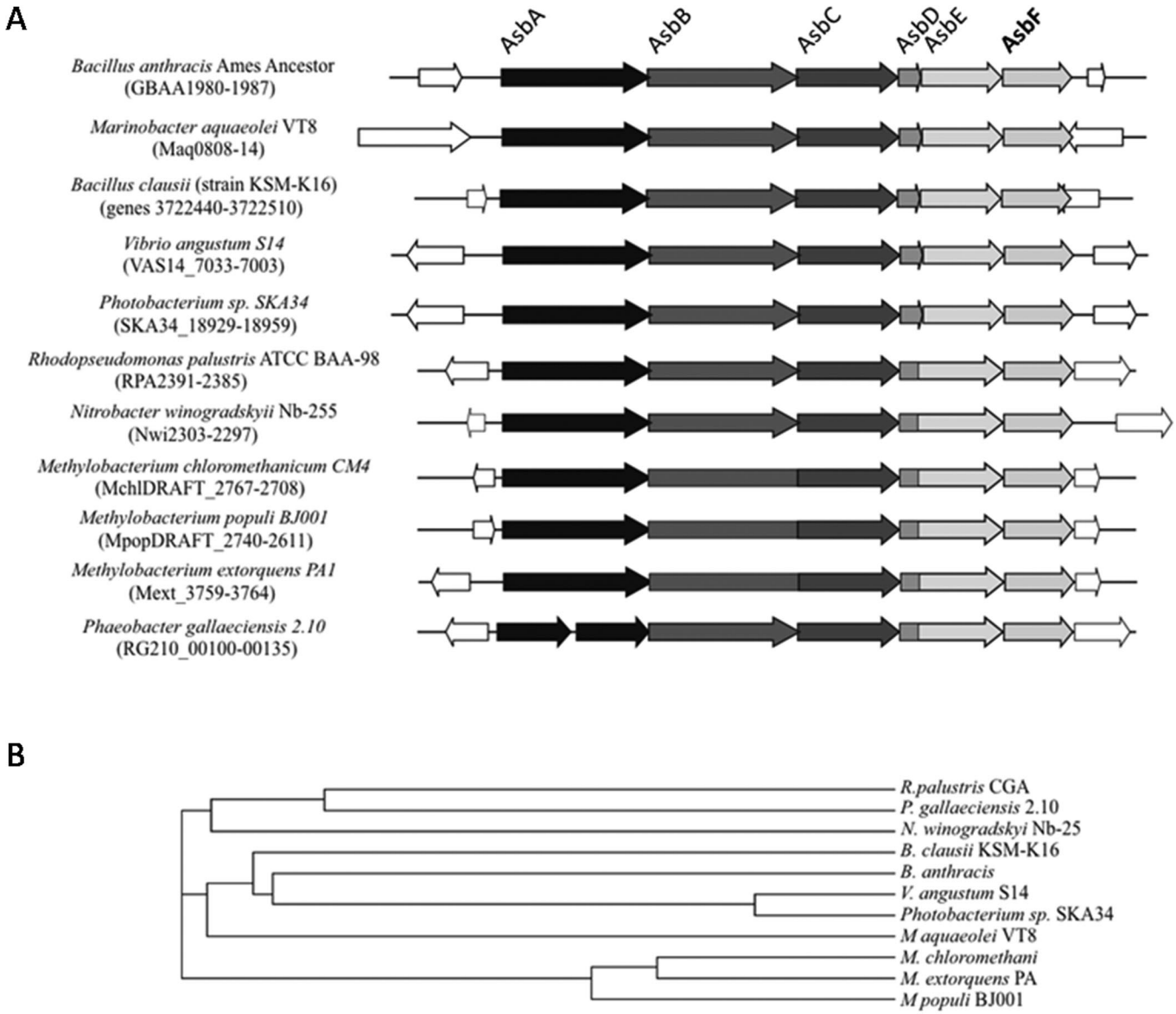

Fig. S2. Conservation of AsbF among diverse prokaryotes. (*A*) Synteny between the *B. anthracis asb* cluster and homologous clusters from other species. The translated *B. anthracis asb* locus (GBAA1981–6, corresponding to *asbA-F*) is shaded and shown at the top, and the corresponding translated loci from each homologous cluster are shown beneath and are shaded to reflect homology with AsbA-F. There is no similarity between genes that are not shaded. (*B*) A cladogram showing the evolutionary relationship (most likely branching order) between AsbF and homologs found in other bacterial genomes. The tree shown was constructed by using the ClustalW server at EBI.

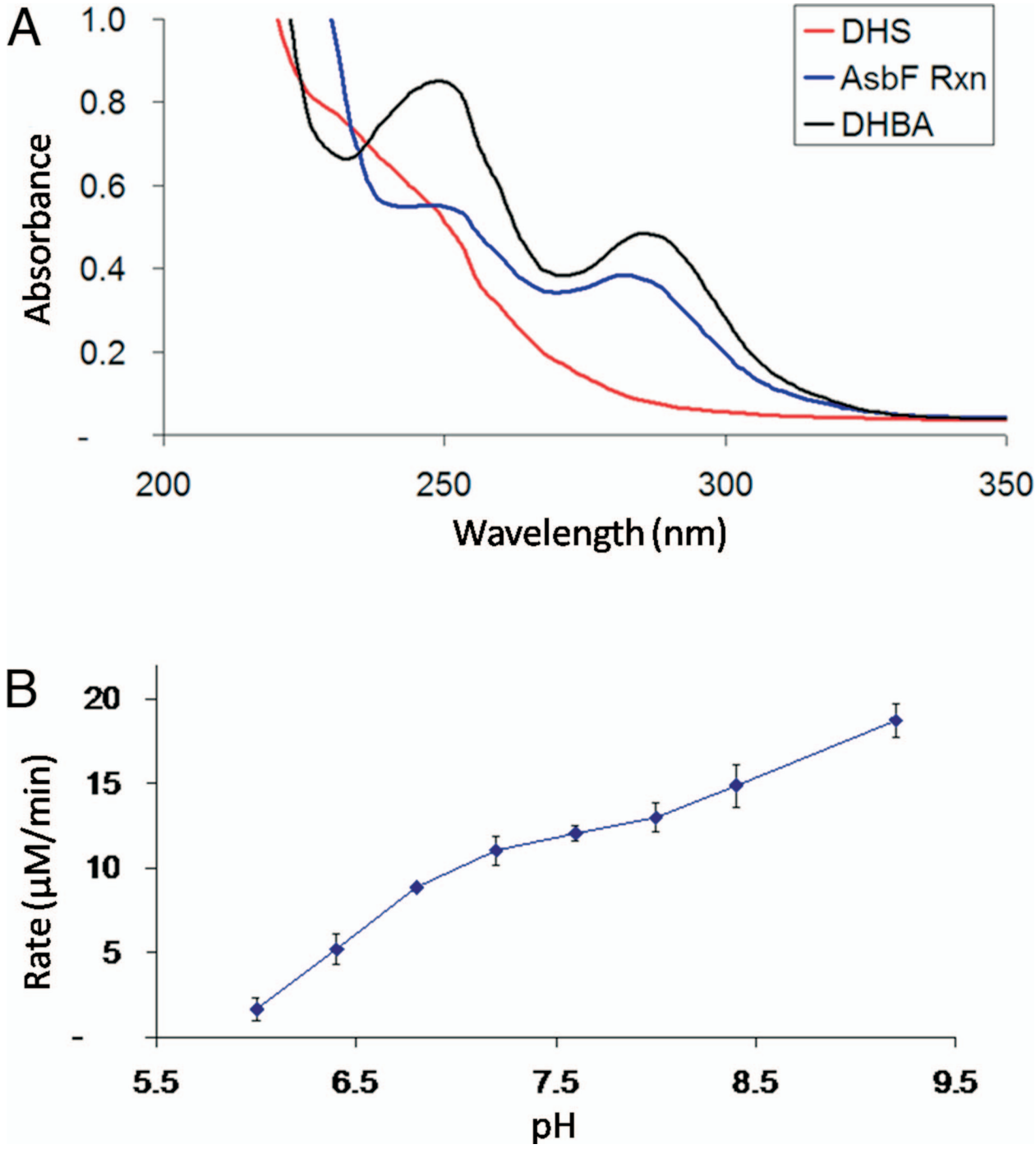

Fig. S3. (*A*) Absorbance spectrum of DHS, DHBA, and AsbF reaction. 3,4-DHBA is highly absorptive at 290 nm whereas, in relation, the 3-DHS substrate and His_6-AsbF enzyme are not. AsbF reaction progression is observed by monitoring at this wavelength. Conditions for the AsbF reaction follow those described in *Materials and Methods*. (*B*) Dependence of the dehydration reaction on pH at 100 mM 3-DHS, 75 mM Hepes, 5 mM $MgCl_2$, and 250 μM AsbF.

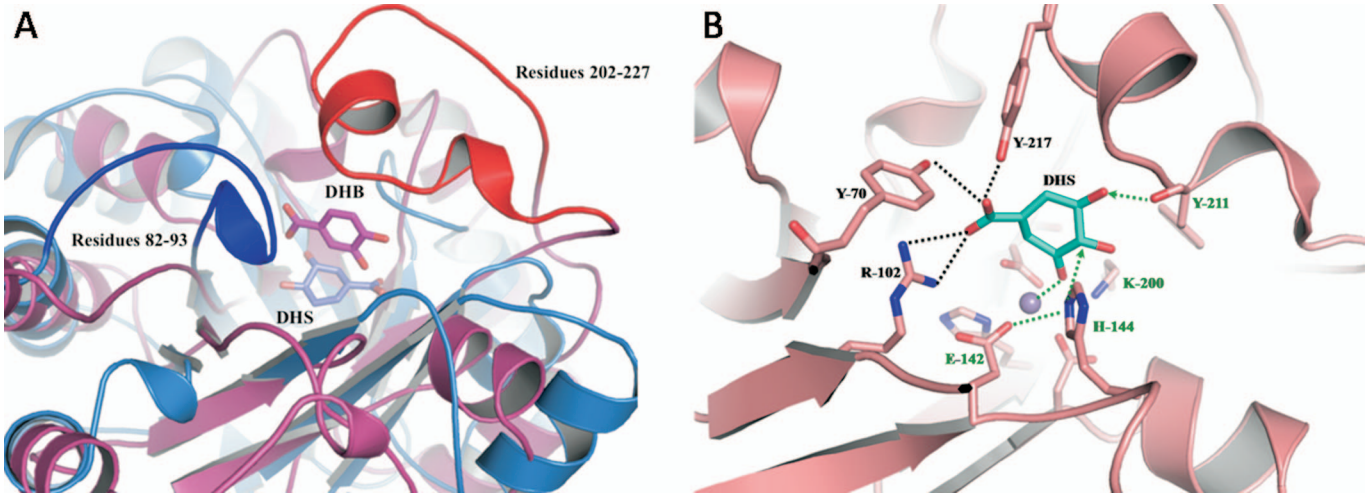

Fig. S4. (*A*) Superposition of the AsbF ribbon (pink) drawing with the DHQ (1qfe) structure (sky blue). 3,4-DHBA in pink stick and 3-DHS in blue are also presented. The lid loops are highlighted in red (for AsbF) and blue (for 1qfe). The 3,4-DHBA molecule in AsbF is located near the top of the pocket right under the lid loop with the aromatic ring facing the barrel wall whereas the dehydroshikimate molecule in DHQ is placed flat at the lower part of the pocket where the H198 side chain resides in the AsbF structure. The carboxylate of 3,4-DHBA is held by the R102 and two tyrosine residues Y217 and Y70, whereas R82 of DHQ occupies the analogous position of AsbF R102 interacting with C4 OH of DHS in the pocket. The carboxylate of DHS is also found to interact with R213 in DHQ. (*B*) 3-DHS molecule is modeled (cyan) in the AsbF binding pocket in approximate place of 3,4-DHBA. Green dashed arrows indicate potential catalytic activities, and potential catalytic residues are shown in green.

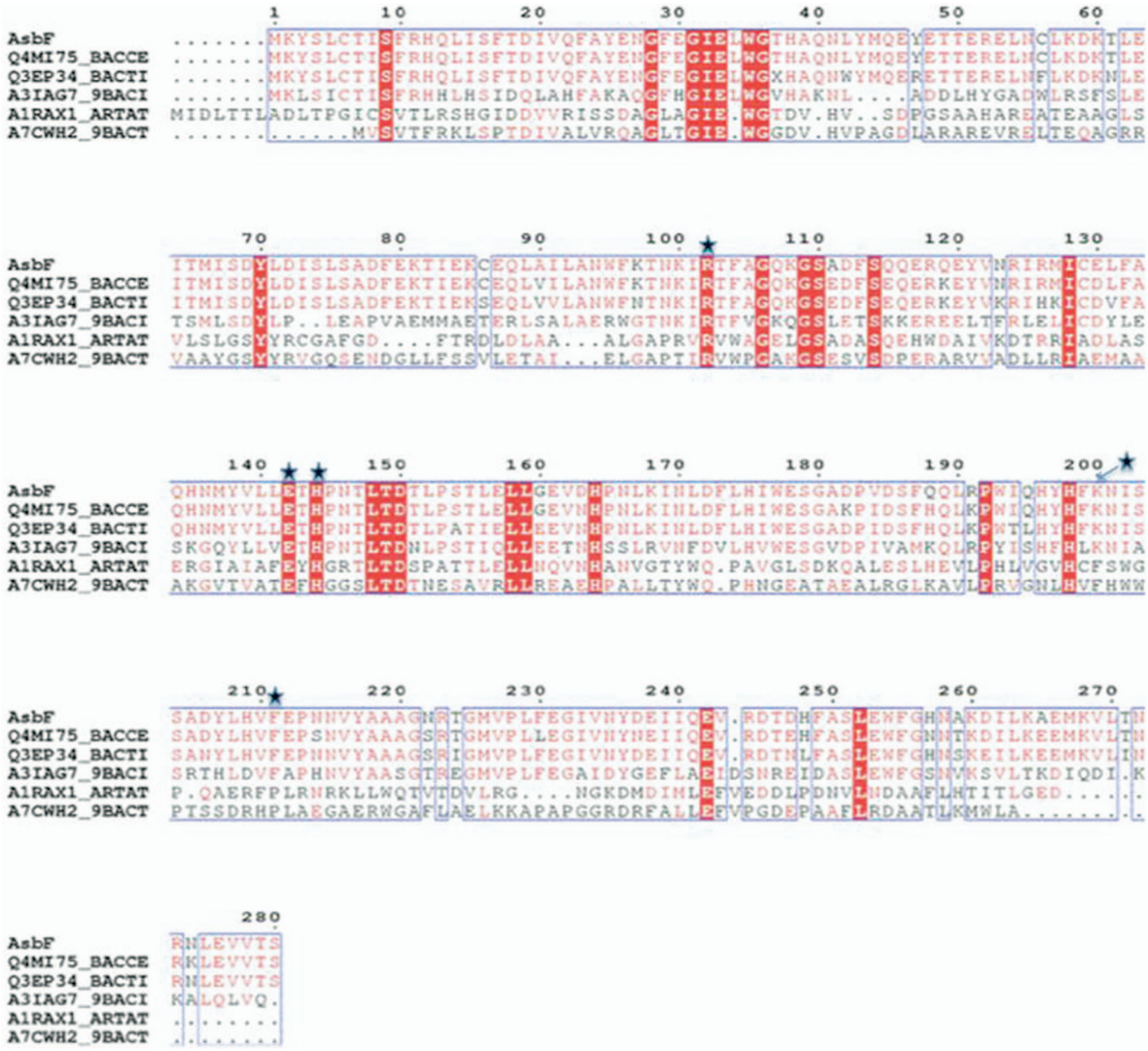

Fig. S5. AsbF with homologous proteins in sequence. Conserved residues are indicated in red; red blocks indicate highest homology. Potential catalytic residues are indicated as asterisks at the top of the residues. Q4MI75_BACCE, putative uncharacterized protein *from B. cereus*; Q3EP34_BACTI, uncharacterized cytosolic protein from *B. thuringiensis serovar israelensis* ATCC 35646; A3IAG7_9BACI, putative uncharacterized protein from *Bacillus* sp. B14905; A1RAX1_ARTAT, putative AP endonuclease, family 2 protein *Arthrobacter aurescens*; A7CWH2_9BACT, xylose isomerase domain protein TIM barrel, *Opitutaceae bacterium TAV2.*

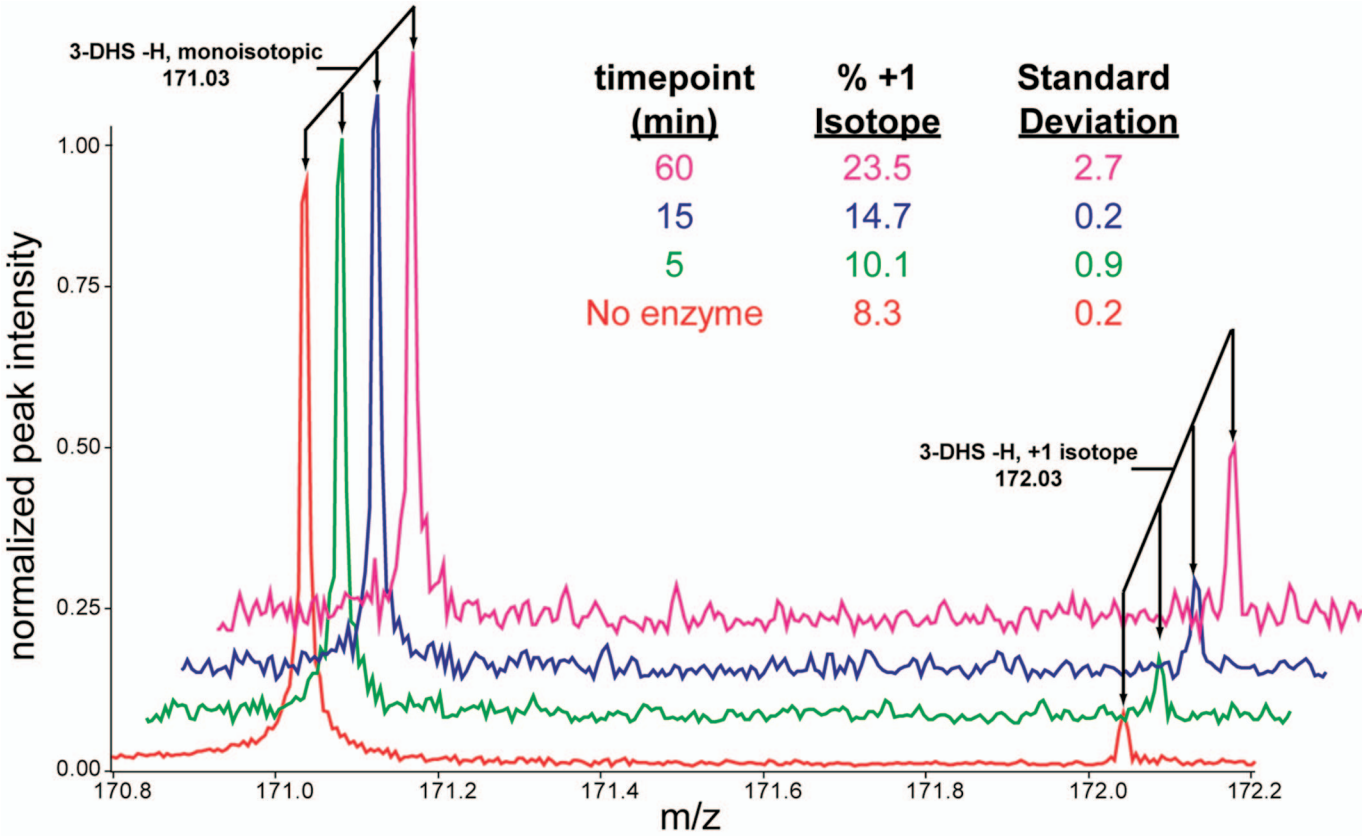

Fig. S6. AsbF-catalyzed D_2O exchange of 3-DHS. One-hundred-microliter deuterium exchange reactions were run with 10 mM Hepes, 1 mM 3-DHS (from a stock dissolved previously in D_2O), and 1 μM AsbF (presoaked in D_2O at 4 °C for 15 min). The reaction was started with the addition of enzyme and quenched at designated time points by acidification with 0.5 μL of formic acid and immediate extraction with ethyl acetate. Reactions were then dried under N_2 and stored at −20 °C. Immediately before Fourier transform ion cyclotron resonance MS (FT-ICR MS) analysis, samples were resuspended in 50:50 IPA:H_2O. The extracted 3-DHS samples were analyzed by an FT-ICR MS (APEX-Q with Apollo II ion source and actively shielded 7T magnet; Bruker Daltonics). Data were gathered from *m/z* 50–1,000 using direct infusion electrospray ionization in negative ion mode. Electrospray was conducted at 2,000 V with 16 scans per spectra using 1-s external ion accumulation in the hexapole before analysis in the FT-ICR using a loop value of 3. Data analysis was performed in Data Analysis (Bruker Daltonics). The monoisotopic peak for 3-DHS at 171.03 Da corresponding to the hydroxyl-deprotonated form in negative mode is readily observed. Because all time points were normalized to the monoisotopic peak, an increase in intensity over time is observed at the +1 isotope peak, corresponding to increasing incorporation of a nonexchangeable deuterium. These data are supported with the numerical values observed and tight standard deviations with triplicate samples. Because 3-DHS is irreversibly converted to 3,4-DHBA because of aromatization, the overall intensity of the 3-DHS peaks does decrease with time (data not shown), even as the monoisotopic and +1 peak ratios shift.

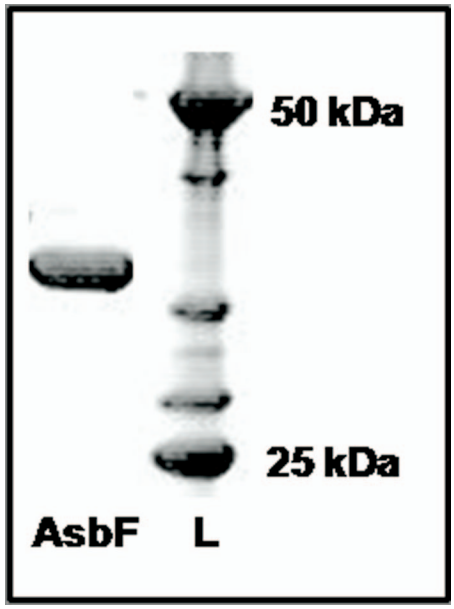

Fig. S7.

Table S1. 3,4-DHBA from *B. anthracis* mutants

Strains	3,4-DHBA, μg/mL IDM supernatant
Sterne $34F_2$	152.25 ± 18.43
Δ*asbA*	457.70 ± 38.61
Δ*asbB*	359.22 ± 42.60
Δ*asbC*	306.03 ± 28.18
Δ*asbD*	239.64 ± 31.02
Δ*asbE*	304.38 ± 29.79
Δ*asbF*	0.09 ± 0.01
Δ*asbABCDEF*	0.07 ± 0.02

Quantification of 3,4-DHBA from supernatants of *Bacillus anthracis asb* mutant cultures. Samples were analyzed by HPLC using a C18 reverse phase semipreparative column (SymmetryPrep C18, 7 μM, 7.8 × 300 mm, Waters). HPLC was performed on a Beckman Coulter System with a diode-array detector using a linear stepwise gradient from 10% to 100% aqueous acetonitrile in 0.1% (vol/vol) trifluoroacetic acid (TFA) at a flow rate of 1.5 mL/min over 40 min for 3,4-DHBA analysis. The retention time and UV spectrum of the corresponding 3,4-DHBA HPLC peaks in each sample were compared with an authentic 3,4-DHBA standard (Sigma). Peak areas were determined and compared with a standard curve constructed by injecting a series of six concentrations (ranging from 0 to 500 μg/mL) of authentic 3,4-DHBA for quantification.